Statistical Thermodynamics of Polymer Solutions

Isaac C. Sanchez*

Center for Materials Science, National Measurement Laboratory, National Bureau of Standards, Washington, D.C. 20234

Robert H. Lacombe

IBM Corporation, Hopewell Junction, New York 12533. Received July 12, 1978

ABSTRACT: The lattice fluid theory of solutions is used to calculate heats and volumes of mixing, lower critical solution temperatures, and the enthalpic and entropic components of the chemical potential. Results of these calculations are compared with literature data on several polyisobutylene solutions. In most instances the agreement with experiment is favorable and comparable to that obtained with the Flory equation of state theory. Several insights into polymer solution behavior are obtained and include: (1) differences in equation of state properties of the pure components make an unfavorable entropic contribution to the chemical potential that becomes large and dominant as the gas–liquid critical temperature of the solvent is approached; (2) limited miscibility of nonpolar polymer solutions at low and high temperatures is a manifestation of a polymer solution's small combinatorial entropy; and (3) negative heats of mixing in nonpolar polymer solutions are caused by the solvent's tendency to contract when polymer is added. Suggestions on how the theory can be improved are made.

Freeman and Rowlinson[1] in 1960 observed that several hydrocarbon polymers dissolved in hydrocarbon solvents phase separated at high temperatures. These nonpolar polymer solutions exhibited what are known as lower critical solution temperatures (LCST), a critical point phenomenon that is relatively rare among low molecular weight solutions. Soon after the discovery of the universality of LCST behavior in polymer solutions, Flory and co-workers[2-5] developed a new theory of solutions which incorporated the "equation of state" properties of the pure components. This new theory of solutions, hereafter referred to as the Flory theory, demonstrated that mixture thermodynamic properties depend on the thermodynamic properties of the pure components and that LCST behavior is related to the dissimilarity of the equation of state of properties of polymer and solvent. Patterson[6-9] has also shown that LCST behavior is associated with differences in polymer/solvent properties by using the general corresponding states theory of Prigogine and collaborators.[10] Classical polymer solution theory, i.e., Flory–Huggins theory,[11] which ignores the equation of state properties of the pure components, completely fails to describe the LCST behavior.

More recently, a new equation of state theory of pure fluids[12,13] and their solutions[14] has been formulated by the present authors. This theory has been characterized as an Ising or lattice fluid theory (hereafter referred to as the lattice fluid (LF) theory). Both the Flory and LF theories require three equation of state parameters for each pure component. For mixtures, both reduce to the Flory–Huggins theory[11] at very low temperatures.

Our general objective in the present paper is to survey the applicability of LF theory to polymer solutions.

Pure Lattice Fluid Properties

As its name suggests, LF theory is founded on a lattice model description of a fluid. An example of such a system is shown in Figure 1. For this model the primary statistical mechanical problem is to determine the number of configurations available to a system of N molecules each of which occupies r sites (an r-mer) and N_0 vacant sites (holes). A mean field approximation is used to solve this problem.[12] In this approximation random mixing of the r-mers with each other and with the vacant sites is assumed. This allows for the evaluation of pair and higher

order probabilities in terms of singlet probabilities; the singlet probabilities are known and are equal to the fraction of each species in the system.

To within an additive constant, the chemical potential μ is given by[12]

$$\mu = rN\epsilon^*\left[-\tilde{\rho} + \tilde{P}\tilde{v} + \tilde{T}\tilde{v}\left[(1 - \tilde{\rho})\ln(1 - \tilde{\rho}) + \frac{\tilde{\rho}}{r}\ln\tilde{\rho}\right]\right] \tag{1}$$

where $\tilde{T}$, $\tilde{P}$, $\tilde{v}$, and $\tilde{\rho}$ are the reduced temperature, pressure, volume, and density defined as

$$\tilde{T} \equiv T/T^*; \quad T^* = \epsilon^*/k \tag{2}$$

$$\tilde{P} \equiv P/P^*; \quad P^* = \epsilon^*/k \tag{3}$$

$$\tilde{v} \equiv 1/\tilde{\rho} \equiv V/V^*; \quad V^* = N(rv^*) \tag{4}$$

and ϵ^* is the interaction per mer and v^* is the close-packed mer volume.

At equilibrium the chemical potential is at a minimum and satisfies the following equation of state:

$$\tilde{\rho}^2 + \tilde{P} + \tilde{T}[\ln(1 - \tilde{\rho}) + (1 - 1/r)\tilde{\rho}] = 0 \tag{5}$$

In general there are three solutions to the equation of state. The solutions at the lowest and highest values of $\tilde{\rho}$ yield minimum values in the chemical potential eq 1, while the intermediate value of $\tilde{\rho}$ produces a maximum in the free energy. The high-density minimum (few vacant sites) corresponds to a liquid phase while the low-density minimum corresponds to a gas or vapor phase (most sites are empty). Typically near the triple point, reduced liquid densities are between 0.7 and 0.9 and gas densities between 0.001 and 0.005. At a given pressure there will be a unique temperature at which the two minima are equal. This temperature and pressure are the *saturation* temperature and pressure and the locus of all such T,P points defines the saturation or coexistence line where liquid and vapor are in equilibrium.

As the saturation temperature and pressure increase, the difference in densities between liquid and vapor phase diminishes until a temperature and pressure are reached where the densities of the two phases are equal. This unique point in the T,P plane is the liquid–vapor critical point (T_c, P_c). For the lattice fluid, the critical point in
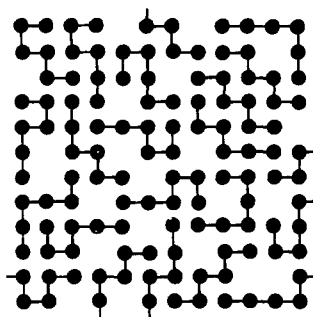
Figure 1. A two-dimensional example of a pure lattice fluid. Hexamers are distributed over the lattice, but not all sites are occupied. The fraction of sites occupied is denoted by $\tilde{\rho}$.
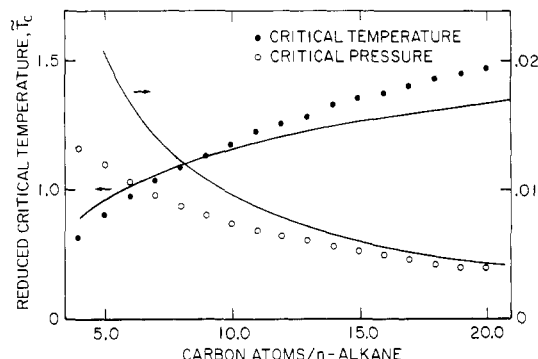

Figure 2. A comparison of the reduced theoretical (solid lines) and experimental critical temperature and pressure for the normal alkanes. In calculating the theoretical curves from eq 7 and 8, the molecular weight per mer was taken to be that of a CH_2 group. The characteristic temperature T^* (520 K) and pressure P^* (280 MN/m²) used to reduce the experimental critical data (API Research Project 44) were chosen as described in the text.

reduced variables is a unique function of the r-mer size. It is given by[12]

$$\tilde{\rho}_c = 1/(1 + r^{1/2}) \tag{6}$$

$$\tilde{T}_c = 2r\tilde{\rho}_c{}^2 \tag{7}$$

$$\tilde{P}_c = \tilde{T}_c[\ln (1 + r^{-1/2}) + (\tfrac{1}{2} - r^{1/2})/r] \tag{8}$$

An examination of the above equations shows that $\tilde{T}_c$ increases with r while $\tilde{P}_c$ and $\tilde{\rho}_c$ decrease with r. Below the critical point and along an isobar, a saturation temperature also increases with r. Thus, for a homologous series of fluids in which we expect T^* and P^* to be relatively constant (see later), the theory predicts that the critical temperature should increase, the critical pressure should decrease, and the normal boiling point should increase with increasing chain length. This type of critical point behavior is exemplified by the normal alkanes as shown in Figure 2. It is the only theory to our knowledge which qualitatively correlates critical and boiling points with chain length.

Another interesting aspect of the critical point is that $\tilde{P}_c \rightarrow 0$ as $r \rightarrow \infty$. For the infinite chain there is only one solution to the equation of state and a phase transition from liquid to vapor is not possible. Stated another way, the equilibrium vapor pressure of the infinite chain is zero.

Determination of the Molecular Parameters. A real fluid is completely characterized by three molecular parameters ϵ^*, v^*, and r or the three equation of state parameters T^*, P^*, and ρ^*. The relationships among these parameters are

$$\epsilon^* = kT^* \tag{9}$$

$$v^* = kT^*/P^* \tag{10}$$

$$r = MP^*/kT^*\rho^* = M/\rho^*v^* \tag{11}$$

Table I
Molecular and Equation of State Parameters [See eq 9, 10, and 11 (1 bar = 0.1 MN/m²)]

	T^*, K	v^*, cm³/mol	r	P^*, MN/m²	ρ^*, kg/m³
methane	224	7.52	4.26	248	500
ethane	315	8.00	5.87	327	640
propane	371	9.84	6.50	314	690
n-butane	403	10.40	7.59	322	736
isobutane	398	11.49	7.03	288	720
n-pentane	441	11.82	8.09	310	755
isopentane	424	11.45	8.24	308	765
neopentane	415	12.97	7.47	266	744
cyclopentane	491	10.53	7.68	388	867
n-hexane	476	13.28	8.37	298	775
cyclohexane	497	10.79	8.65	383	902
n-heptane	487	13.09	9.57	309	800
n-octane	502	13.55	10.34	308	815
n-nonane	517	14.00	11.06	307	828
n-decane	530	14.47	11.75	305	837
$n\text{-}C_{11}H_{24}$	542	14.89	12.40	303	846
$n\text{-}C_{12}H_{26}$	552	15.28	13.06	300	854
$n\text{-}C_{13}H_{28}$	560	15.58	13.79	299	858
$n\text{-}C_{14}H_{30}$	570	15.99	14.36	296	864
$n\text{-}C_{17}H_{36}$	596	17.26	15.83	287	880
benzene	523	9.8	8.02	444	994
flourobenzene	527	10.39	8.05	422	1150
chlorobenzene	585	11.14	8.38	437	1210
bromobenzene	608	11.13	8.73	454	1620
toluene	543	11.22	8.50	402	966
p-xylene	561	12.24	9.14	381	949
m-xylene	560	12.11	9.21	384	952
o-xylene	571	12.03	9.14	395	965
CCl_4	535	11.69	7.36	381	1790
$CHCl_3$	512	9.33	7.58	456	1690
CH_2Cl_2	487	7.23	7.64	560	1540

In principle any thermodynamic property can be utilized to determine these parameters, but saturated vapor pressure data are particularly useful because they are readily found in the literature for a wide variety of fluids. Equation of state parameters have been determined for 60 different fluids by a nonlinear least-squares fitting of experimental vapor pressure data.[12] A partial listing is shown in Table I. An alternative method for determining the parameters is discussed in Appendix A.

For a polymer liquid $r \rightarrow \infty$ and the equation of state reduces to a simple corresponding states equation:

$$\tilde{\rho}^2 + \tilde{P} + \tilde{T}[\ln (1 - \tilde{\rho}) + \tilde{\rho}] = 0 \tag{12}$$

Equation of state parameters can be determined for polymers by a nonlinear least-squares fit of eq 12 to experimental liquid density data.[13] Figure 3 illustrates the corresponding states behavior of several polymer liquids over a large temperature and pressure range. The lines are theoretical isobars calculated from eq 12 at the indicated reduced pressures; $\tilde{P} = 0$ is essentially atmospheric pressure and $\tilde{P} = 0.25$ is of the order of a 100 MN/m². The various symbols are the reduced experimental density data. Table II lists the equation of state parameters for the polymers represented in Figure 3.

In cases where limited PVT data are available for a given polymer, the equation of state parameters can be estimated from experimental values of density, thermal expansion coefficient, and compressibility determined at the same temperature and atmospheric pressure.[13]

Physical Interpretation of the Molecular Parameters

In our original publication,[12] we identified ϵ^* with a nearest neighbor mer interaction energy. However, it is

Table II
Equation of State Parameters for Some Common Polymers

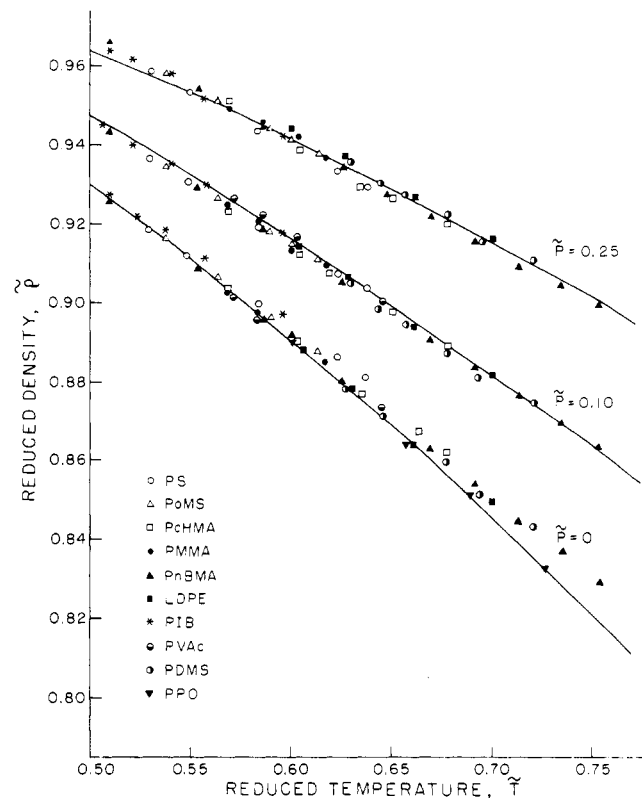|		T^*, K	P^*, MN/m²	v^*, cm³/mol	ρ^*, kg/m³	temp range, K	pressures up to, MN/m²
poly(dimethylsiloxane)	PDMS	476	302	13.1	1104	298–343	100
poly(vinyl acetate)	PVAC	590	509	9.64	1283	308–373	80
poly(n-butyl methacrylate)	PnBMA	627	431	12.1	1125	307–473	200
polyisobutylene	PIB	643	354	15.1	974	326–383	100
polyethylene (linear)	HDPE	649	425	12.7	904	426–473	100
polyethylene (branched)	LDPE	673	359	15.6	887	408–471	100
poly(methyl methacrylate)	PMMA	696	503	11.5	1269	397–432	200
poly(cyclohexyl methacrylate)	PcHMA	697	426	13.6	1178	396–472	200
polystyrene (atatic)	PS	735	357	17.1	1105	388–468	200
poly(2,6-dimethylphenylene oxide)	PPO	739			1186	493–533	0
poly(o-methylstyrene)	PoMS	768	378	16.9	1079	412–471	160

Figure 3. Graphical illustration of the corresponding states behavior of several common polymer liquids. The lines are theoretical isobars calculated from eq 12. Experimental density data were reduced by the equation of state parameters listed in Table II.

not necessary to do so and below we generalize its meaning: the total configurational potential energy, E, of the LF can be expressed quite generally as

$$E = \frac{1}{2}(rN)\bar{\varepsilon} \tag{13}$$

$$\bar{\varepsilon} = 4\pi\rho \int_0^\infty \varepsilon(R)g(R)R^2 \, dR \tag{14}$$

where $\bar{\varepsilon}$ is the average interaction energy of a mer with all other mers in the system, $\varepsilon(R)$ is the intermolecular potential between mers separated by a distance R, $g(R)$ is the pair distribution function, and ρ is the mer density in mers per unit volume. Let us assume a Sutherland type potential (hard core plus attractive tail) for the interaction between mers; i.e.,

$$\varepsilon(R) = \infty \text{ for } (R/v^{*1/3}) < 1 \tag{15}$$

$$\varepsilon(R) = -\varepsilon_0(v^{*1/3}/R)^n \text{ for } (R/v^{*1/3}) > 1$$

For a hard core potential in the mean field approximation, the pair distribution function is given by

$$g(R) = 0 \text{ for } (R/v^{*1/3}) < 1 \tag{16}$$

$$g(R) = 1 \text{ for } (R/v^{*1/3}) > 1$$

Substitution of eq 15 and 16 into eq 14 and 13 yields

$$E = -rN\varepsilon^*\tilde{\rho} \tag{17}$$

$$\varepsilon^* = 2\pi\varepsilon_0/(n - 3) \tag{18}$$

For the usual value of $n = 6$, $\varepsilon^* = 2\pi\varepsilon_0/3$. Thus, ε^* is proportional to the depth of the potential energy well.

The important point of the above calculation is that in the mean field approximation, the fluid potential energy is of the van der Waals type (proportional to fluid density) if the intermolecular potential is sufficiently short range ($n > 3$).

LF theory is intended to describe the fluid (disordered) and not the crystalline (ordered) state even though a lattice is used in the formulation of the theory. In keeping with this view, the close-packed state should be disordered, more akin to the glassy state than the crystalline state. Disordered close packing is not as dense as ordered close packing. A well-known example of this effect occurs with spheres. The packing fraction P_f, the fraction of space occupied, for closest packing of spheres (hexagonal or face-centered cubic) is 0.74 while P_f for *random* close packing is 0.637.[15] When the close-packed densities (ρ^*) listed in Table I are compared with known crystalline densities, it is found that most of the ρ^* densities are smaller (usually about 10%). Thus, we can identify rv^* (see eq 11) with the *close-packed molecular volume* of the disordered fluid.

It is also instructive to examine the variation in rv^* and $r\varepsilon^*$ for the normal alkanes. Between C_3 and C_{14}, rv^* increases from one member to the next by 15.0 ± 0.4 cm³/mol. This suggests that each CH_2 group contributes a constant amount to the molecular close-packed volume. This conclusion is further reinforced by plotting the close-packed mass density ρ^* against reciprocal chain length. A relatively straight line is obtained which can be extrapolated to infinite chain length where $\rho^* = 934$ kg/m³. From this value we also conclude that the close-packed volume of a CH_2 group is $14.0/0.934 = 15.0$ cm³/mol. The ρ^* value of linear polyethylene from Table II is, however, 904 kg/m³ which yields a close-packed volume of a CH_2 group of $14.0/0.904 = 15.5$ cm³/mol. Considering that the molecular parameters for polyethylene were determined from density data and those for the normal alkanes from vapor pressure data, the agreement between the calculated close-packed volumes is quite satisfactory.

The total molecular interaction energy is $r\varepsilon^*$ which equals the energy required to convert 1 mol of the fluid

from the close-packed state ($\tilde{\rho} = 1$) to a vapor of vanishing density ($\tilde{\rho} = 0$). From Table I, $\epsilon^* = kT^*$ is seen to increase irregularly with chain length for the normal alkanes, but the increase in $r\epsilon^*$ between C_3 and C_{14} is much more systematic. It increases at 4.35 ± 0.6 kJ/mol of CH_2 which suggests that a CH_2 unit contributes a nearly constant amount to the total molecular interaction energy.

The above values of 15.0 cm^3/mol for the close-packed volume and 4.35 kJ/mol for the close-packed interaction energy of a CH_2 group yield $T^* = 520$ K and $P^* = 280$ MN/m^2. These parameters were used to prepare Figure 2. The r value for each alkane was determined by dividing its molecular weight by 14.

The identification of $r\epsilon^*$ with the energy of vaporization in the close-packed state allows for a simple interpretation of the ratio ϵ^*/v^*. This ratio is defined as the characteristic pressure P^* and is equal to the cohesive energy density (CED) of the fluid in the close-packed state since CED $\equiv \Delta E_{vap}/V = r\epsilon^*/rv^* \equiv P^*$. At finite temperatures CED = $\tilde{\rho}^2 P^*$ if we ignore the interactions in the vapor phase (always true at zero pressure). Thus, P^* is a direct measure of the "cohesiveness" of the fluid or the strength of the intermolecular interactions.

Mixed Lattice Fluids

Combining Rules. Extension of the LF theory to mixtures is relatively straightforward after the appropriate "combining rules" are adopted. Such rules are required in all statistical mechanical theories of mixtures and are often quite arbitrary. For the mixed LF model, one reason that combining rules become necessary is that each pure component has its own unique mer volume v^*_i whereas in the mixture all mers are required to have the same *average* close-packed volume v^* (hereafter, unsubscripted variables refer to the mixture). The combining rules as stated below all refer to the properties of a close-packed mixture: (1) If an i molecule occupies r_i^0 sites in the pure state and has a close-packed molecular volume of $r_i^0 v^*_i$, then it will occupy r_i sites in the mixture such that

$$r_i^0 v_i^* = r_i v^* \tag{19}$$

This rule guarantees simple additivity of the close-packed volumes:

$$V^* = r_1^0 N_1 v_1^* + r_2^0 N_2 v_2^* = (r_1 N_1 + r_2 N_2) v^* \tag{20}$$

(2) The total number of *pair interactions* in the close-packed mixture is equal to the sum of the pair interactions of the components in their close-packed pure states, i.e.,

$$(z/2)(r_1^0 N_1 + r_2^0 N_2) = (z/2)(r_1 N_1 + r_2 N_2) = (z/2)rN \tag{21}$$

where z is the coordination number of the lattice and

$$r \equiv x_1 r_1^0 + x_2 r_2^0 \equiv x_1 r_1 + x_2 r_2 \tag{22}$$

$$x_1 \equiv N_1/N = 1 - x_2 \text{ (mole fraction)} \tag{23}$$

$$N \equiv N_1 + N_2 \tag{24}$$

(3) Characteristic pressures are pairwise additive in the close-packed mixtures:

$$P^* = \phi_1 P_1^* + \phi_2 P_2^* - \phi_1 \phi_2 \Delta P^* \tag{25}$$

$$\Delta P^* \equiv P_1^* + P_2^* - 2P_{12}^* \tag{26}$$

$$\phi_1 = r_1 N_1/rN = 1 - \phi_2 \tag{27}$$

The first two combining rules yield the following relationship for the average close-packed mer volume:

$$v^* = \phi_1^0 v_1^* + \phi_2^0 v_2^* \tag{28}$$

where

$$\phi_1^0 = r_1^0 N_1/rN = 1 - \phi_2^0 \tag{29}$$

The concentrations ϕ_1 and ϕ_1^0 are related by

$$\phi_1^0 = \frac{\phi_1}{\phi_1 + \nu\phi_2}; \quad \phi_1 = \frac{\nu\phi_1^0}{\nu\phi_1^0 + \phi_2^0} \tag{30}$$

$$\nu \equiv v_1^*/v_2^* \tag{31}$$

From the definition of ϕ_i given in eq 27 and the first combining rule, it can be easily shown that it represents the *close-packed volume fraction* of component i; i.e.,

$$\phi_1 = \frac{m_1/\rho_1^*}{m_1/\rho_1^* + m_2/\rho_2^*} \tag{32}$$

where m_1 and m_2 are the respective *mass fractions*. In subsequent equations, concentrations will always be expressed in terms of ϕ_i.

The volume of the mixture is

$$V = (N_0 + rN)v^* = V^*\tilde{v} \tag{33}$$

Alternatively, the reduced volume $\tilde{v}$ can be expressed in terms of the specific volume of the mixture v_{sp} or its mass density ρ:

$$\tilde{v} = v_{sp}/v_{sp}^* = \rho^*/\rho = 1/\tilde{\rho} \tag{34}$$

where

$$v_{sp}^* = m_1/\rho_1^* + m_2/\rho_2^* = 1/\rho^* \tag{35}$$

In our original specification of the combining rules,[12] only eq 19 and 21 were imposed. Here we add a third rule, eq 25. Adding this rule does not introduce additional theoretical parameters; adding this third rule, however, yields a more quantitative theory.

The old combining rules yielded pairwise additivity of the mer–mer interaction energies ϵ_{ij} [cf. eq 27 of ref 14]. We have shown that the characteristic pressure P^* is closely related to the physical property of cohesive energy density and our third rule insures pairwise additivity of this property in the close-packed state. Now the mer–mer interaction energy of the mixture ϵ^* is given by

$$\epsilon^* = P^* v^* = \\ (\phi_1 P_1^* + \phi_2 P_2^* - \phi_1 \phi_2 \Delta P^*)(\phi_1^0 v_1^* + \phi_2^0 v_2^*) \tag{36}$$

and will only be pairwise additive when $v_1^* = v_2^*$. Thus, under the new rules P^* is pairwise additive and ϵ^* is not, whereas under the old rules ϵ^* was pairwise additive and P^* was not. Further justification of eq 36 is given in Appendix C.

It is convenient to introduce reduced variables. The reduced volume and density are defined by eq 34 and the reduced temperature $\tilde{T}$ and pressure $\tilde{P}$ of the mixture are defined formally as before:

$$\tilde{T} = T/T^*; \quad T^* = \epsilon^*/k \tag{37}$$

$$\tilde{P} = P/P^*$$

where ϵ^* is given by eq 36 and P^* is given by eq 25. From eq 36 and 30, T^* can be expressed as

$$T^*/T \equiv 1/\tilde{T} = [\phi_1/\tilde{T}_1 + \nu\phi_2/\tilde{T}_2]/(\phi_1 + \nu\phi_2) - \phi_1\phi_2 X \tag{38}$$

where

$$X \equiv \Delta P^* v^*/kT \tag{39}$$

Free Energy and Chemical Potentials. The configurational Gibbs free energy G of a binary mixture is given by (cf. eq 1):

$$G \equiv rN\epsilon^*\tilde{G} \tag{40}$$

$$\tilde{G} = -\tilde{\rho} + \tilde{P}\tilde{v} + \tilde{T}\tilde{v}\left[(1-\tilde{\rho})\ln(1-\tilde{\rho}) + \frac{\tilde{\rho}}{r}\ln\tilde{\rho}\right] + \tilde{T}\left[\frac{\phi_1}{r_1}\ln\phi_1 + \frac{\phi_2}{r_2}\ln\phi_2\right] \tag{41}$$

Minimization of the free energy with respect to density or volume yields the same equation of state as before, eq 5, but with T^*, P^*, and r defined as above (r is also given by $1/r = \phi_1/r_1 + \phi_2/r_2$).

The chemical potential μ_1 is

$$\mu_1 \equiv \left.\frac{\partial G}{\partial N_1}\right|_{T,P,N_2} \tag{42}$$

$$\mu_1 = kT[\ln\phi_1 + (1 - r_1/r_2)\phi_2 + r_1^0\tilde{\rho}X_1\phi_2^2] + r_1^0kT\left\{-\tilde{\rho}/\tilde{T}_1 + \tilde{P}_1\tilde{v}/\tilde{T}_1 + \tilde{v}\left[(1-\tilde{\rho})\ln(1-\tilde{\rho}) + \frac{\tilde{\rho}}{r_1^0}\ln\tilde{\rho}\right]\right\} \tag{43}$$

where X_1 is given by

$$X_1 \equiv X(\phi_1 = 1) = \Delta P^* v_1^*/kT \tag{44}$$

The expression for μ_2 is easily obtained by interchanging the indices 1 and 2.

The chemical potentials have the following properties:

(1) They reduce correctly to their appropriate molar pure state values (cf. eq 1):

$$\mu_1(\phi_1 = 1) = \mu_1^0 \tag{45}$$

(2) At low temperatures or high pressures the reduced densities approach their maximum value of unity. In this limit the Flory-Huggins chemical potentials are recovered (as $\tilde{\rho}$ and $\tilde{\rho}_1 \rightarrow 1$)

$$(\mu_1 - \mu_1^0)/kT \rightarrow \ln\phi_1 + (1 - r_1/r_2)\phi_2 + r_1^0X_1\phi_2^2 \tag{46}$$

(3) There is only one parameter, ΔP^* or X_1, that characterizes a binary mixture. All other parameters are known from the pure components. It is convenient to characterize the interaction in terms of a dimensionless parameter ζ which measures the deviation of P_{12}^* from the geometric mean:

$$\zeta = P_{12}^*/(P_1^*P_2^*)^{1/2} \tag{47}$$

and eq 26 becomes

$$\Delta P^* = P_1^* + P_2^* - 2\zeta(P_1^*P_2^*)^{1/2} \tag{48}$$

Mixing Functions. The fractional volume change $\Delta V_m/V_0$ that occurs upon mixing is (V_0 is the "ideal volume" of the mixture assuming additivity):

$$\Delta V_m/V_0 = \tilde{v}/(\phi_1\tilde{v}_1 + \phi_2\tilde{v}_2) - 1 \tag{49}$$

The heat (enthalpy) of mixing ΔH_m at low pressures is ($P\Delta V_m$ term ignored):

$$\Delta H_m/RT = r\{\tilde{\rho}\phi_1\phi_2X + v^*[\phi_1P_1^*(\tilde{\rho}_1 - \tilde{\rho}) + \phi_2P_2^*(\tilde{\rho}_2 - \tilde{\rho})]/RT\} \tag{50}$$

The entropy of mixing ΔS_m is

$$\Delta S_m/R = -r\left\{\frac{\phi_1}{r_1}\ln\phi_1 + \frac{\phi_2}{r_2}\ln\phi_2 + \tilde{v}\left[(1-\tilde{\rho})\ln(1-\tilde{\rho}) + \frac{\tilde{\rho}}{r}\ln\tilde{\rho}\right]\right\} + \frac{r}{\phi_1 + \nu\phi_2}\left\{\phi_1\tilde{v}_1\left[(1-\tilde{\rho}_1)\ln(1-\tilde{\rho}_1) + \frac{\tilde{\rho}_1}{r_1^0}\ln\tilde{\rho}_1\right] + \nu\phi_2\tilde{v}_2\left[(1-\tilde{\rho}_2)\ln(1-\tilde{\rho}_2) + \frac{\tilde{\rho}_2}{r_2^0}\ln\tilde{\rho}_2\right]\right\} \tag{51}$$

The first two terms in ΔS_m are the Flory-Huggins combinatorial entropy terms.

Phase Stability and the Spinodal. A negative free energy of mixing is a necessary but not sufficient condition for miscibility. For a binary mixture at a given temperature and pressure, a necessary and sufficient condition for miscibility over the entire composition range is for $d\mu_1/dx_1$ to be positive over the entire range ($d\mu_2/dx_2$ will also be positive through a Gibbs-Duhem relation). Under these conditions the free energy of mixing is also negative as required.

This positive property of the chemical potentials is related to the *curvature* properties of the intensive free energy $g \equiv G/N$ of the binary mixture:

$$\mu_1 \equiv \left.\frac{\partial G}{\partial N_1}\right|_{T,P,N_2} = g + x_2\frac{dg}{dx_1} \tag{52}$$

$$\frac{d\mu_1}{dx_1} = x_2\frac{d^2g}{dx_1^2} \tag{53}$$

Thus, $d\mu_1/dx_1 > 0$ implies $d^2g/dx_1 > 0$ or that the Gibbs free energy per mole of mixture (at constant T and P) is a *convex* function of composition.

For a binary LF mixture at constant temperature and pressure, we have

$$\frac{d(\mu_1/kT)}{d\phi_1} = 2r_1\phi_2\left\{\frac{1}{2}\left[\frac{1}{r_1\phi_1} + \frac{1}{r_2\phi_2}\right] - \tilde{\rho}\left[X + \frac{1}{2}\psi^2\tilde{T}P^*\beta\right]\right\} \tag{54}$$

where ψ is a dimensionless function defined by

$$\psi \equiv \tilde{\rho}\frac{d(1/\tilde{T})}{d\phi_1} - \frac{d(1/r)}{d\phi_1} + \tilde{v}\frac{d(\tilde{P}/\tilde{T})}{d\phi_1} \tag{55a}$$

$$\psi = \left\{\tilde{\rho}[\nu(1/\tilde{T}_1 - 1/\tilde{T}_2) + (\phi_1^2 - \nu\phi_2^2)X_1] - \nu(1/r_1^0 - 1/r_2^0) + \frac{\tilde{P}\tilde{v}}{\tilde{T}}(\nu - 1)(\phi_1 + \nu\phi_2)\right\}/(\phi_1 + \nu\phi_2)^2 \tag{55b}$$

and β is the isothermal compressibility of the mixture given by

$$\tilde{T}P^*\beta = \tilde{v}[1/(\tilde{v} - 1) + 1/r - 2/\tilde{v}\tilde{T}]^{-1} > 0 \tag{56}$$

Therefore, g is convex and miscibility is possible if the following inequality holds:

$$\frac{1}{2}\left[\frac{1}{r_1\phi_1} + \frac{1}{r_2\phi_2}\right] - \tilde{\rho}\left[X + \frac{1}{2}\psi^2\tilde{T}P^*\beta\right] > 0 \tag{57}$$

where $[(1/r_1\phi_1) + (1/r_2\phi_2)]$ is the combinatorial entropy contribution, $\tilde{\rho}X$ is an energetic contribution and $^1/_2\tilde{\rho}\psi^2\tilde{T}P^*\beta$ is an entropic contribution from equation of state. *It is significant to note that the entropic equation of state term makes an unfavorable contribution to the*
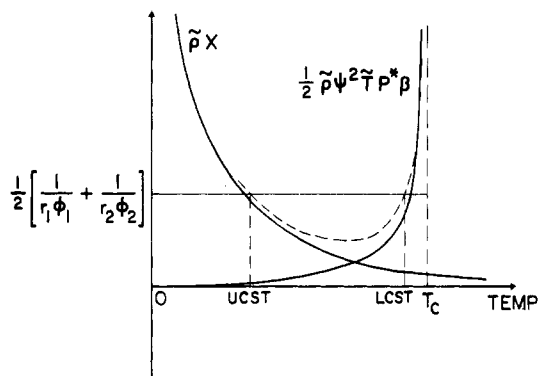
Figure 4. Schematic behavior of the three terms in the spinodal inequality 57 as a function of temperature. The dashed curve is the sum $\tilde{\rho}X + {}^{1}/_{2}\psi^{2}TP^{*}\beta$. The inequality is satisfied between the UCST and LCST.

spinodal, i.e., its presence does not favor miscibility.

If the spinodal inequality is not satisfied, a binary fluid mixture is thermodynamically unstable and will phase separate into two fluid phases. (We do not rule out the possibility of phase separation in a dense gas mixture.) The boundary separating the one-phase and two-phase regions is called the spinodal and is defined by the condition $d\mu_{1}/d\phi_{1} = 0$.

In most cases the general character of the equilibrium liquid–liquid phase diagram can be deduced by studying the spinodal. (The equilibrium phase diagram is defined by the condition that the chemical potential of each component is the same in both phases.) To illustrate this, consider a binary liquid mixture that is closed to the atmosphere and in equilibrium with its vapor. In this closed system the pressure equals the equilibrium vapor pressure of the mixture. Let us further assume that X is positive. The temperature dependence of the three terms in the spinodal inequality 57 is illustrated in Figure 4. Only $\tilde{\rho}X$ and the equation of state term $\tilde{\rho}\psi^{2}\tilde{T}P^{*}\beta$ are temperature dependent. The entropic equation of state term diverges as the liquid–vapor critical temperature T_{c} of the mixture is approached ($P \rightarrow P_{c}$) because $\beta \rightarrow \infty$ at T_{c}. Notice that the inequality is only satisfied over a finite temperature interval (suggests an upper and lower critical solution temperature); i.e., miscibility is theoretically possible only in a finite temperature range. If the composition is changed, the line representative of the combinatorial entropy term in Figure 4 moves up or down and miscibility is obtained over a different temperature range. For $\nu = 1$, the minimum value of the combinatorial entropy term occurs at

$$\phi_{1}^{m} = \frac{1}{1 + (r_{1}/r_{2})^{1/2}} \qquad (58)$$

Since the other two terms in the spinodal inequality are, by comparison, weak functions of composition, the critical composition ϕ_{1}^{c} for both the UCST and LCST will *approximately* equal ϕ_{1}^{m}.

In a polymer/solvent system $r_{2} \gg r_{1}$ and $\phi_{1}^{m} \rightarrow 1$; the temperature–composition (T–ϕ) phase diagram becomes very distorted and the critical point occurs when the solution is very dilute in polymer ($\phi_{2} \simeq 0$). Under these conditions the stability condition implies that miscibility for dilute solutions requires that the second virial coefficient of the chemical potential be positive:

$$(\mu_{1}^{0} - \mu_{1})/kT = \frac{r_{1}}{r_{2}}\phi_{2} + \left(\frac{1}{2} - \chi_{1}\right)\phi_{2}^{2} + \left(\frac{1}{3} - \chi_{2}\right)\phi_{2}^{3} + \dots \qquad (59)$$
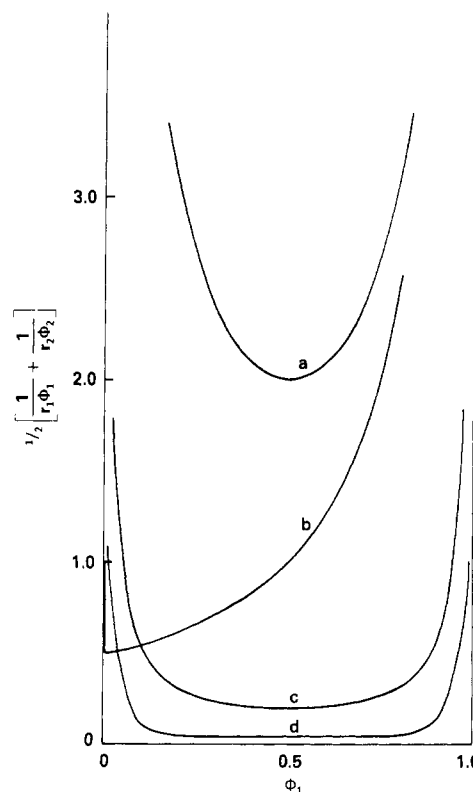

Figure 5. Combinatorial entropy contribution to the spinodal vs. close-packed volume fraction ϕ_{1}. Curve a, $r_{1} = r_{2} = 1$; curve b, $r_{1} = 1$, $r_{2} \gg 1$; curve c, $r_{1} = r_{2} = 10$; and curve d, $r_{1} = r_{2} = 50$.

For a polymer solution near a critical point, $\phi_{2}/r_{2} \sim r_{2}^{-3/2}$ and $\phi_{2}^{2} \sim r^{2-1}$ by eq 58, and therefore, the second-order term dominates

$$(\mu_{1}^{0} - \mu_{1})/kT \simeq ({}^{1}/_{2} - \chi_{1})\phi_{2}^{2} \qquad (60)$$

Now $d\mu_{1}/d\phi_{1} > 0$ implies that $({}^{1}/_{2} - \chi_{1}) > 0$ for stability in dilute solutions. For the LF, we have (see Appendix B):

$$\chi_{1} = r_{1}^{0}\tilde{\rho}_{1}[X_{1} + {}^{1}/_{2}\psi_{1}^{2}\tilde{T}_{1}P_{1}^{*}\beta_{1}] \qquad (61)$$

where $\psi_{1} \equiv \psi$ ($\phi_{1} = 1$) and ψ is defined by eq 55. It is easy to show that r_{1} times the spinodal inequality equals ${}^{1}/_{2} - \chi_{1}$ for $r_{2}/r_{1} \gg 1$ and $\phi_{1} = \phi_{1}^{m}$.

According to LF theory, every closed binary system in equilibrium with its own vapor is capable of exhibiting LCST behavior prior to reaching its liquid–vapor critical temperature T_{c}. In low molecular weight solutions, the combinatorial entropy term is relatively large and the LCST should appear very close to T_{c} where it may be difficult to observe experimentally. In contrast, for a polymer solution the combinatorial entropy term is small (see Figure 5) and the LCST can occur well below the critical temperature of the solvent. For many polyisobutylene/solvent systems $0.7 < \text{LCST}/T_{c} < 0.9$.[17]

Comparison of Theory and Experiment

Heats and Volumes of Mixing. The LF theory is a one-parameter theory of a binary mixture. This parameter ΔP^{*} (or the related parameters X_{1} and ζ) can be determined from a single solution datum. Here we use heats of mixing at infinite dilution.

When the solvent (component 1) is in excess ΔH_{m} approaches a limiting value $\Delta H_{m}(\infty)$ given by

$$\Delta H_{m}(\infty) \equiv \lim_{\phi_{2} \rightarrow 0} \Delta H_{m}/\phi_{2} \equiv \frac{d\Delta H_{m}}{d\phi_{2}}\bigg|_{\phi_{2}=0} \qquad (62)$$

Table III
Interaction Parameters Calculated from Heats of Mixing for Dilute Polyisobutylene Solutions

	$\tilde{\rho}_1$	$\tilde{T}_1$	$P_1^*\beta_1$	$\Delta H_m(\infty)$, J/mol	$X_1 \times 10^2$	ΔP^*, MJ/m³	ζ	ψ_1
n-pentane	0.820	0.676	0.804	−201	4.980	10.4	0.9864	−0.491
n-hexane	0.852	0.626	0.595	−159	3.238	6.04	0.9944	−0.497
n-heptane	0.864	0.612	0.522	−100	2.594	4.91	0.9949	−0.460
n-octane	0.875	0.594	0.462	−67	2.128	3.89	0.9965	−0.440
n-decane	0.893	0.562	0.379	−31	1.438	2.46	0.9991	−0.393
cyclohexane	0.868	0.600	0.507	−38	2.442	5.61	0.9932	−0.365
benzene	0.882	0.570	0.441	1090	8.180	20.7	0.9803	−0.239

In units of energy/mole of repeat unit, the LF theory yields:

$$\Delta H_m(\infty)/RT = r_1{}^0(M_u/M_1)(\rho_1^*/\rho_2^*) \times$$
$$[\tilde{\rho}_1 X_1 + \tilde{\rho}_1{}^2 \psi_1 P_1^*\beta_1 + \nu(\tilde{\rho}_2 - \tilde{\rho}_1)/\tilde{T}_2] \quad (63)$$

where M_u is the molecular weight of the polymer repeat unit and M_1 is the solvent molecular weight. In deriving eq 63 we used the important relation

$$d\tilde{\rho}/d\phi_1 = \tilde{\rho}^2 \psi \tilde{T} P^* \beta \quad (64)$$

Table III contains experimental values of $\Delta H_m(\infty)$ at 298 K for seven polyisobutylene (PIB) solutions[18] and the corresponding values of X_1 calculated from eq 63. Also shown are ΔP^* and ζ obtained from X_1 via eq 44 and 48. A striking feature of the data is that six of these nonpolar polymer solutions are exothermic. Notice, however, that all of the calculated X_1 values are positive.

Inspection of eq 63 reveals the physical principles that determine the sign of $\Delta H_m(\infty)$. The first term, $\tilde{\rho} X_1$, is the exchange interaction energy parameter. A positive X_1 should, according to classical theory, yield a positive ΔH_m because it is proportional to the net change in energy that accompanies the formation of a 1–2 bond from a 1–1 and a 2–2 bond. The term proportional to $(\tilde{\rho}_2 - \tilde{\rho}_1)$ is also positive since $\tilde{\rho}_2 > \tilde{\rho}_1$ for all solutions in Table III. This term is associated with the process of taking a polymer molecule out of a high-density medium $(\tilde{\rho}_2)$ and placing it in one of lower density $(\tilde{\rho}_1)$; this is energetically less favorable and contributes positively to $\Delta H_m(\infty)$. The remaining term, $\tilde{\rho}_1{}^2 \psi_1 P_1^* \beta_1$, has a similar interpretation with respect to the solvent molecules. This term can be positive or negative depending on the sign of $\psi_1 = \psi$ ($\phi_1 = 1$). The sign of ψ_1 (see eq 55) is largely determined by the sign of $(T_1^* - T_2^*)$ and as can be seen in Table III is negative in all cases. From eq 64 this implies that $d\tilde{\rho}/d\phi_2 > 0$ at $\phi_2 = 0$ or adding a small amount of polymer to solvent causes a *density contraction*. The magnitude of the contraction is proportional to the compressibility of the solvent (β_1). It is energetically favorable because at a distance R from a given solvent mer, there are now more mers/unit volume and the average interaction is stronger $(T_2^* > T_1^*)$. It is this term that dominates $\Delta H_m(\infty)$ for six of the seven solutions in Table III.

Also notice that all solutions with a negative ΔH_m also yield negative volume changes[5,19–21] although a negative ΔV_m is not a sufficient condition for a negative ΔH_m. The quoted values of ΔV_m are the maximum observed volume changes which all occur near the 50:50 composition (by weight). The calculated values of ΔV_m based on the interaction parameters determined from $\Delta H_m(\infty)$ data are not in very good agreement. However, the correct signs are obtained and the deviations are systematic.

Although benzene has a large and positive heat of mixing with PIB at room temperature, it decreases with increasing temperature and finally becomes negative near 435 K.[22] Figure 6 compares the experimental (solid circles) and
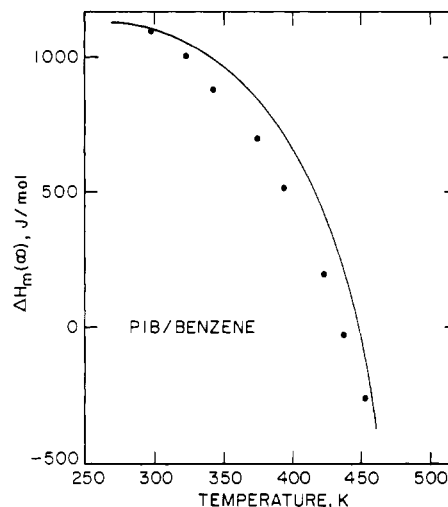

Figure 6. A comparison of experimental[22] (solid circles) and theoretical (solid line) heats of mixing for dilute solutions of polyisobutylene in benzene. The theoretical curve was calculated from eq 63 using temperature-independent pure-component parameters from Tables I and II.

calculated (solid line) ΔH_m (∞) as a function of temperature. The theoretical curve was calculated using *temperature independent* pure component parameters and the value of the interaction parameter determined at 298 K. As can be seen, the agreement is quite good.

Chemical Potentials. A more stringent test of theory is to compare chemical potentials using the interaction parameters shown in Table III. For the purposes of comparison it is convenient to define the activity of the solvent (a_1) in terms of a dimensionless χ parameter:

$$(\mu_1 - \mu_1{}^0)/RT \equiv \ln a_1 = \ln \phi_1 + \phi_2 + \chi \phi_2{}^2 \quad (65)$$

This functional form is that suggested by classical theory (we have set $r_1/r_2 = 0$; cf. eq 46) in which χ is inversely proportional to temperature and independent of concentration. It is now well known that χ does not possess a simple $1/T$ dependence and in general is concentration dependent. Empirical values of χ as a function of concentration are obtained from measured activities by solving eq 65 for χ.[23] Defined in this way χ may be called the *reduced residual chemical potential*.[5]

Similarly, we can define a reduced *residual enthalpy* and *entropy* of dilution by

$$\chi_H \equiv -T(\partial\chi/\partial T) \quad (66)$$

$$\chi_S \equiv \partial(T\chi)/\partial T \quad (67)$$

and, of course,

$$\chi = \chi_H + \chi_S \quad (68)$$

The quantities χ_H and χ_S correspond to κ and $1/2 - \psi$ in Flory's older notation.[11]

Table IV
Comparison of Experimental and Theoretical Chemical Potentials, Volumes of Mixing, and Lower Critical Solution Temperatures for Polyisobutylene Solutions at 298 K

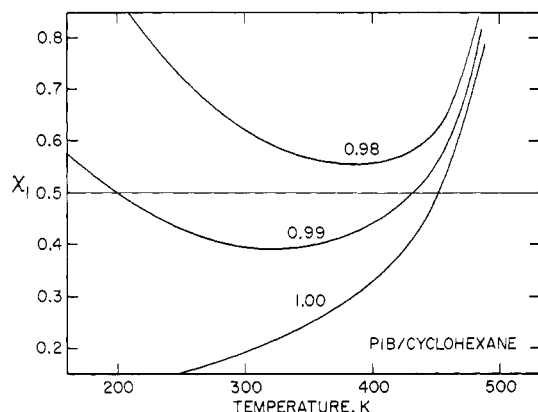|	χ_1		$\chi_{H;1}$		$\chi_{S;1}$		χ^∞		$\Delta V_m/V_0 \times 10^2$		Θ_s, K	
	exptl	calcd	exptl	calcd	exptl	calcd	exptl	calcd	exptl	calcd	exptl	calcd
n-pentane	0.49	0.76	−0.42	−0.33	0.91	1.09	0.93	0.69	−1.27	−1.83	344	
n-hexane		0.56		−0.27		0.83		0.47	−0.857	−1.25	402	
n-heptane		0.49		−0.18		0.67		0.43	−0.615	−0.92	442	303
n-octane	0.46	0.43	−0.17	−0.13	0.63	0.57	>0.5	0.38	−0.481	−0.73	477	375
n-decane		0.32		−0.09		0.41		0.28	−0.291	−0.48	535	470
cyclohexane	0.47	0.34	0.00	−0.02	0.47	0.36	0.5	0.36	−0.14	−0.44	516	440
benzene	0.50	0.63	0.26	0.67	0.24	−0.04	1.15	0.74	0.34	0.20	534	487

Figure 7. The variation of the reduced chemical potential χ_1 as a function of temperature for polyisobutylene/cyclohexane solution at the indicated values of the interaction parameter ζ (see eq 48). Notice how strongly χ_1 depends on ζ at low temperatures.

The concentration dependence of these quantities can be expressed formally in series form:

$$\chi = \chi_1 + \chi_2\phi_2 + \chi_3\phi_2^2 + \ldots \tag{69}$$

$$\chi_H = \chi_{H;1} + \chi_{H;2}\phi_2 + \ldots$$

$$\chi_S = \chi_{S;1} + \chi_{S;2}\phi_2 + \ldots \tag{70}$$

The coefficients χ_i are the same coefficients in the virial expansion of the chemical potential shown in eq 59. The limiting values of these parameters are particularly important:

$$\chi(\phi_1 = 1) \equiv \chi_1 = \chi_{H;1} + \chi_{S;1} \tag{71}$$

$$\chi(\phi_1 = 0) \equiv \chi^\infty = \chi_H^\infty + \chi_S^\infty = \sum_1^\infty \chi_i \tag{72}$$

For the LF, χ_1 is given by eq 61 and χ^∞ by

$$\chi^\infty = r_1^0 \left[\tilde{p}_2 X_1 + (\tilde{p}_1 - \tilde{p}_2)/\tilde{T}_1 + (\tilde{v}_2 - 1) \times \right.$$

$$\left. \ln(1 - \tilde{p}_2) - (\tilde{v}_1 - 1) \ln(1 - \tilde{p}_1) + \frac{1}{r_1^0} \ln(\tilde{p}_2/\tilde{p}_1) \right] \tag{73}$$

Experimental[5,19-21,24] and calculated values of χ_1, $\chi_{H;1}$, $\chi_{S;1}$, and χ^∞ are shown in Table IV for four PIB solutions. Notice the large and positive (unfavorable) value of $\chi_{S;1}$ for pentane, octane, and cyclohexane solutions ($\chi_{S;1} = 0$ in classical theory). That the good agreement is not fortuitous can better be appreciated by studying Figures 7 and 8. The calculated values are often sensitive functions of temperature and the interaction parameter. In Figure 7, χ_1 is plotted as a function of temperature at three different values of the interaction parameter (ζ) for PIB/cyclohexane. Notice how strongly χ_1 depends on ζ at room temperatures. In Figure 8 χ_1, $\chi_{H;1}$, and $\chi_{S;1}$ are
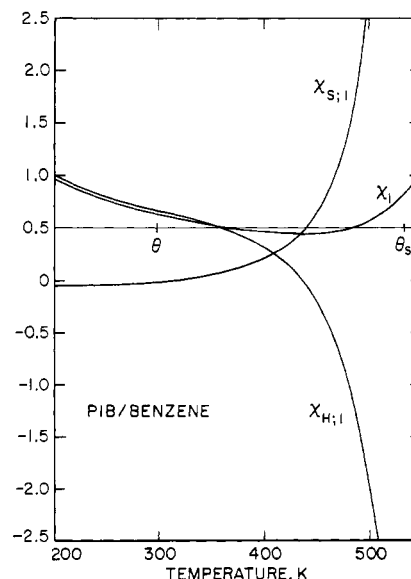

Figure 8. The variation of χ_1 and its enthalpic $\chi_{H;1}$ and entropic $\chi_{S;1}$ components with temperature are illustrated for dilute polyisobutylene/benzene solutions with $\zeta = 0.9803$.

shown as a function of temperature for PIB/benzene for $\zeta = 0.9803$. As the LCST is approached, $\chi_{H;1}$ and $\chi_{S;1}$ individually diverge rapidly in opposite directions, whereas their sum, χ_1, diverges more slowly in the positive direction.

Critical Temperatures. When compared to similar low molecular weight solutions, polymer solutions are anomalous in two respects: First, limited miscibility is often observed at room temperatures even when polymer and solvent are both nonpolar, and second, polymer solutions show a greater propensity for phase separation at high temperatures. Complete miscibility is obtained above the upper critical solution temperature (UCST), and below the LCST. Both the UCST and LCST depend on molecular weight. With increasing molecular weight, the UCST approaches a limiting value called the Θ temperature.[11] Similarly, the LCST approaches an asymptotic limit with molecular weight.[25-27] We shall refer to the LCST Θ as the *superus* Θ and designate it as Θ_s.

Stability conditions lead to the following conditions on χ_1 (cf. previous section on phase stability):

$$\chi_1 = \frac{1}{2} \text{ for } T = \Theta \text{ or } \Theta_s$$

$$\chi_1 < \frac{1}{2} \text{ for } \Theta < T < \Theta_s$$

$$\chi_1 > \frac{1}{2} \text{ for } T < \Theta \text{ or } T > \Theta_s$$

Therefore, Θ and Θ_s can easily be located by calculating χ_1 as a function of temperature. In Figure 8 χ_1 is plotted as a function of temperature for PIB/benzene and yields $\Theta = 370$ K and $\Theta_s = 487$ K as compared to the experimental values of $\Theta = 298$ K and $\Theta_s = 534$ K.[17] The calculated values are based on $\zeta = 0.9803$. If ζ is increased

to 0.9864, $\Theta = 298$ K and $\Theta_s = 490$ K. Although Θ is relatively sensitive to the interaction parameter, Θ_s is not as can be seen in Figure 7 for PIB/cyclohexane. Actually no value of ζ can be chosen to yield a theoretical Θ_s of 534 K. The entropic equation of state term, which is jointly proportional to the compressibility of the solvent (β_1) and ψ_1^2, dominates χ_1 at high temperatures (see eq 61). In all of our calculations, the calculated Θ_s is less than the observed value (see Table IV). This seems to indicate that $\chi_{S;1}$ is overestimated at high temperatures.

Summary and Conclusions

A general result of the LF theory is that differences in equation of state properties of the pure components make a thermodynamically unfavorable entropic contribution to the chemical potential. This is most apparent in the stability condition (the spinodal inequality 57) where the positive term $\bar{\rho}\psi^2\tilde{T}P^*\beta$ can be shown to be completely entropic. This term is only zero at $T = 0$ or when $\psi = 0$; ψ is a function of pure component parameter differences (see eq 55) and is in general nonzero. Thus, differences in pure component parameters, especially T^* values, tend to destabilize a solution and make it more susceptible to phase separation. This unfavorable entropic term, which is small and relatively unimportant at low temperatures, becomes large and dominant as the liquid–gas critical temperature T_c is approached (see Figure 4). In both low molecular weight and polymer solutions this term is similar in magnitude, but the favorable contribution that the combinatorial entropy makes toward stability is much smaller for polymer solutions. This small combinatorial entropy term makes a polymer solution more susceptible to phase separation (than a similar low molecular weight solution) at both low and high temperatures. Therefore, we reach the general conclusion that in nonpolar polymer solutions *limited miscibility at low and high temperatures is a manifestation of a polymer solution's small combinatorial entropy.*

Heats of mixing at infinite dilution $\Delta H_m(\infty)$ have been used to determine the interaction energy parameter between polyisobutylene and seven hydrocarbon solvents. The interaction parameter can be expressed in any of three equivalent forms, X_1, ΔP^*, and ζ, and all are tabulated in Table III. The parameter ΔP^* physically represents the net change in cohesive energy density upon mixing at the absolute zero of temperature. As might be expected for these nonpolar solutions, the calculated ΔP^*'s are all positive. Thus, at absolute zero the heats of mixing would all be positive (endothermic). However, only PIB/benzene has a positive $\Delta H_m(\infty)$ at 298 K. In terms of the LF theory, negative heats are caused by the tendency of the solvent to contract when a small amount of polymer is added. The magnitude of the contraction is proportional to the isothermal compressibility of the solvent. It is an energetically favorable process because it results in more intermolecular interactions of lower potential energy among the solvent molecules.

Although $\Delta H_m(\infty)$ is large and positive at room temperature for PIB/benzene, it decreases with increasing temperature and becomes exothermic near 435 K. LF theory semiquantitatively accounts for this behavior as shown in Figure 6.

Using the interaction parameters determined from $\Delta H_m(\infty)$ data, volumes of mixing ΔV_m were calculated and tabulated in Table IV. Theory correctly predicts that all of the PIB solutions, except benzene, have negative ΔV_m's. In all cases, including benzene, the calculated solution volume was smaller than observed. The Flory equation of state theory of solutions[5] correlates these volume

changes slightly better than LF theory. In the Flory theory, the pure component parameters were all determined at 298 K whereas in the LF theory these parameters are obtained over a large temperature range. If the LF parameters are chosen so as to perfectly reproduce pure liquid densities at 298 K as in the Flory theory, better agreement with experiment is obtained. However, we prefer not to use temperature-dependent parameters and have not done so in any of the calculations in this paper.

Chemical potentials have been calculated in both dilute and concentrated ranges and compared with available experimental data on PIB solutions of *n*-pentane, *n*-octane, cyclohexane, and benzene as shown in Table IV. The essential validity of theory is manifested in the calculated values of the reduced residual entropy at infinite dilution ($\chi_{S;1}$). In classical theory $\chi_{S;1} = 0$, yet $\chi_{S;1}$ dominates the chemical potential in dilute PIB solutions of *n*-pentane, *n*-octane, and cyclohexane. As can be seen the calculated $\chi_{S;1}$ values are in good agreement with those observed except for benzene.

Notice that negative (favorable) values of the residual enthalpy $\chi_{H;1}$ are associated with positive (unfavorable) values of $\chi_{S;1}$. Qualitatively, this trend can be understood. In a dilute polymer solution the solvent molecules, as explained above, are in a slightly denser environment than in the pure state; this is energetically favorable and promotes negative values of $\chi_{H;1}$. However, entropy decreases with density ($dS/d\rho < 0$) and the denser environment lowers the entropy of the solvent molecules which is thermodynamically unfavorable ($\chi_{S;1} > 0$).

Lower critical solution temperatures have also been calculated and are tabulated in Table IV. For *n*-pentane and *n*-hexane the calculated value of χ_1 is greater than 0.5 and theory incorrectly predicts limited miscibility of PIB in these two solvents at 298 K. (The variation of χ_1 with T for these two systems would be similar to that shown for PIB/cyclohexane in Figure 7 for $\zeta = 1.0$.) For the remaining solvents the calculated LCST's are all lower than observed.

As polymer concentration increases, the reduced residual chemical potential (χ) approaches a limiting value $\chi^\infty \equiv \chi(\phi_1 = 0)$. For most polymer solutions that have been studied, $d\chi/d\phi_2 > 0$ and $\chi_1 \equiv \chi(\phi_1 = 1) < \chi^\infty$. An exception to this trend can be found in polystyrene/chloroform solutions.[28] In Table IV notice that *n*-pentane and benzene solutions of PIB have large and positive experimental values of $d\chi/d\phi_2$ whereas theory yields only a small positive value for benzene and a negative one for *n*-pentane. For PIB/benzene, the variation in χ with ϕ_2 is largely determined by the large positive value of $d\chi_H/d\phi_2$[21] whereas theoretically $d\chi_H/d\phi_2 < 0$ and $d\chi_S/d\phi_2 > 0$. (Similar data for PIB/*n*-pentane are not available.) This is the most serious shortcoming of the LF theory.

In the Flory theory the sign and magnitude of $d\chi/d\phi_2$ is a sensitive function of the s_1/s_2 ratio[4] (s_i is the surface to volume ratio of component i). In principle this ratio can be estimated from molecular models or by using van der Waal values. However, the values obtained by these two methods often differ appreciably as in the case of polystyrene/methyl ethyl ketone.[29] Unlike the Flory theory we have not explicitly introduced surface area corrections via the combining rules into the LF theory.

This brings us finally to an assessment of the future. How can theory be improved? Both the Flory and LF theories employ approximate equations of state to describe the pure component fluids. Better equations of state of the pure components should produce a better theory of solutions.

We can experiment with new combining rules. LF theory seems particularly flexible in this respect compared to Flory's theory. In Appendix C the LF theory is generalized to facilitate experimentation with different sets of combining rules. The quantity that is most affected by the combining rules is the ψ function (defined by eq 55) which is very sensitive to the value of $d\epsilon^*/d\phi_1$. Small changes in ψ, for example, can dramatically affect calculated values of χ_S and χ_H.

There is also the need to make suitable corrections to the theory for dilute polymer solutions. In the dilute regime there is little overlap between polymer molecules and a non-uniform distribution of polymer segments exists, whereas the mean field character of the theory assumes uniformity of the segment distribution.

Appendix A

Molecular parameters for low molecular weight fluids can be estimated from a known heat of vaporization ΔH_v, a vapor pressure P, and a liquid specific volume v_l all at the same temperature T:

$$r = \frac{\Delta H_v/RT - \ln(v_g/v_l)}{1 + (\tilde{v}-1)\ln(1-\tilde{\rho})} \quad (A.1)$$

$$T^* = \epsilon^*/R = (\Delta E_v/R)/r\tilde{\rho} \quad (A.2)$$

$$\rho^* = 1/\tilde{\rho}v_l \quad (A.3)$$

$$v^* = M/r\rho^* \quad (A.4)$$

$$p^* = RT^*/v^* \quad (A.5)$$

The reduced density $\tilde{\rho}$ required above satisfies the following equation which must be numerically evaluated:

$$[2\Delta E_v/RT - \ln(v_g/v_l)][\tilde{\rho} + \ln(1-\tilde{\rho})] - $$
$$[\Delta E_v/RT - 1]\tilde{\rho}\ln(1-\tilde{\rho}) = 0 \quad (A.6)$$

where ΔE_v is the energy of vaporization and v_g is the specific volume of the gas phase.

In deriving the above results we assumed that P was low enough so that the vapor phase could be treated as an ideal gas and that $v_g \gg v_l$. Under these conditions the entropy of vaporization ΔS_v is given by

$$\Delta S_v/R = \Delta H_v/RT = r[1 + (\tilde{v}-1)\ln(1-\tilde{\rho})] + $$
$$\ln(v_g/v_l) \quad (A.7)$$

and

$$\Delta E_v = \Delta H_v - RT = r\tilde{\rho}/\tilde{T} \quad (A.8)$$

Using eq A.7 and A.8, r and $\tilde{T}$ can be eliminated in the equation of state eq 12 to obtain eq A.6 with $\tilde{P} = 0$.

Appendix B

Listed below is a compendium of useful relations for binary mixtures based on the combining rules of this paper, eq 19, 21, and 25.

$$v^* = \frac{v_1^* v_2^*}{\phi_1 v_2^* + \phi_2 v_1^*} = \frac{v_1^*}{\phi_1 + \nu\phi_2} \quad (B.1)$$

$$r_1 = (\phi_1 + \nu\phi_2)r_1^0; \qquad r_2 = (\phi_1 + \nu\phi_2)r_2^0/\nu \quad (B.2)$$

$$\frac{d(1/\tilde{T})}{d\phi_1} = [\nu(1/\tilde{T}_1 - 1/\tilde{T}_2) + (\phi_1^2 - \nu\phi_2^2)x_1]/(\phi_1 + \nu\phi_2)^2 \quad (B.3)$$

$$\frac{d^2(1/\tilde{T})}{d\phi_1^2} = \frac{2\nu}{(\phi_1 + \nu\phi_2)^3}[X_1 + (\nu-1)(1/\tilde{T}_1 - 1/\tilde{T}_2)] \quad (B.4)$$

$$\frac{d(1/r)}{d\phi_1} = \frac{\nu(1/r_1^0 - 1/r_2^0)}{(\phi_1 + \nu\phi_2)^2};$$
$$\frac{d^2(1/r)}{d\phi_1^2} = \frac{2\nu(\nu-1)(1/r_1^0 - 1/r_2^0)}{(\phi_1 + \nu\phi_2)^3} \quad (B.5)$$

$$\frac{d(\tilde{P}/\tilde{T})}{d\phi_1} = \frac{\tilde{P}(\nu-1)}{\tilde{T}(\phi_1 + \nu\phi_2)};$$
$$\frac{d^2(\tilde{P}/\tilde{T})}{d\phi_1^2} = \frac{2\tilde{P}(\nu-1)^2}{\tilde{T}(\phi_1 + \nu\phi_2)^2} \quad (B.6)$$

$$\frac{d\tilde{v}}{d\phi_1} = -\psi\tilde{T}P^*\beta; \qquad \frac{d\tilde{\rho}}{d\phi_1} = \tilde{\rho}^2\psi\tilde{T}P^*\beta \quad (B.7)$$

$$\frac{d\psi}{d\phi_1} = \tilde{\rho}\frac{d^2(1/\tilde{T})}{d\phi_1^2} + \frac{d(1/\tilde{T})}{d\phi_1}\frac{d\tilde{\rho}}{d\phi_1} - \frac{d^2(1/r)}{d\phi_1^2} + $$
$$\tilde{v}\frac{d^2(\tilde{P}/\tilde{T})}{d\phi_1^2} + \frac{d(\tilde{P}/\tilde{T})}{d\phi_1}\frac{d\tilde{v}}{d\phi_1} \quad (B.8)$$

$$\frac{d(\tilde{T}P^*\beta)}{d\phi_1} = \tilde{\rho}(\tilde{T}P^*\beta)^2\left\{[2/\tilde{T} - (1-\tilde{\rho})^{-2}]\frac{d\tilde{\rho}}{d\phi_1} + \right.$$
$$\left. \frac{d(1/\tilde{T})}{d\phi_1} - \tilde{v}\frac{d(\tilde{P}/\tilde{T})}{d\phi_1}\right\} \quad (B.9)$$

$$\frac{d^2\tilde{v}}{d\phi_1^2} = -\left[\psi\frac{d(\tilde{T}P^*\beta)}{d\phi_1} + \tilde{T}P^*\beta\frac{d\psi}{d\phi_1}\right] \quad (B.10)$$

$$\bar{V}_1 \equiv \frac{\partial V}{\partial N_1}\bigg|_{T,P,N_2} = r_1^0 v_1^*\left[\tilde{v} + \phi_2\frac{d\tilde{v}}{d\phi_1}\right] \quad (B.11)$$

$$\chi_H = \frac{r_1^0}{\phi_2^2}\{(\tilde{\rho}_1 - \tilde{\rho})/\tilde{T}_1 + P_1(\tilde{v} - \tilde{v}_1)/\tilde{T}_1 + \tilde{\rho}X_1\phi_2^2\} - $$
$$\frac{r_1\tilde{\rho}^2\psi P^*\beta}{\phi_2} \quad (B.12)$$

$$\chi_S = \frac{r_1^0}{\phi_2^2}\left\{(\tilde{v}-1)\ln(1-\tilde{\rho}) - (\tilde{v}_1-1)\ln(1-\tilde{\rho}_1) + \right.$$
$$\left. \frac{1}{r_1^0}\ln(\tilde{\rho}/\tilde{\rho}_1)\right\} + \frac{r_1\tilde{\rho}^2\psi P^*\beta}{\phi_2} \quad (B.13)$$

$$\chi_H{}^\infty = r_1^0\{(\tilde{\rho}_1 - \tilde{\rho}_2)/\tilde{T}_1 + $$
$$\tilde{P}_1(\tilde{v}_2 - \tilde{v}_1)/\tilde{T}_1 + \tilde{\rho}_2X_1 - \nu\tilde{\rho}_2^2\psi_2P_2^*\beta_2\} \quad (B.14)$$

$$\chi_S{}^\infty = r_1^0\left\{(\tilde{v}_2-1)\ln(1-\tilde{\rho}_2) - (\tilde{v}_1-1)\ln(1-\tilde{\rho}_1) + \right.$$
$$\left. \frac{1}{r_1^0}\ln(\tilde{\rho}_2/\tilde{\rho}_1) + \nu\tilde{\rho}_2^2\psi_2P_2^*\beta_2\right\} \quad (B.15)$$

where

$$\psi_2 \equiv \psi(\phi_2 = 1) \quad (B.16)$$

$$\chi^\infty = \chi_H{}^\infty + \chi_S{}^\infty \quad (B.17)$$

$$\chi_{H;1} = r_1^0(\tilde{\rho}_1X_1 + R_1) \quad (B.18)$$

$$\chi_{S;1} = r_1^0(\tilde{\rho}_1\psi_1^2\tilde{T}_1P_1^*\beta_1 - R_1) \quad (B.19)$$

where

$$R_1 = \tilde{\rho}_1 \left.\frac{d\tilde{v}}{d\phi_1}\right|_{\phi_1=1} \left\{ \tilde{\rho}_1[\nu/\tilde{T}_2 - 1/\tilde{T}_1 - X_1] + \right.$$

$$\left. \frac{\tilde{\rho}_1^2}{\tilde{T}_1} \left.\frac{d\tilde{v}}{d\phi_1}\right|_{\phi_1=1} \right\} - \frac{1}{2}[(\tilde{\rho}_1^2 + \tilde{P}_1)/\tilde{T}_1] \left.\frac{d^2\tilde{v}}{d\phi_1^2}\right|_{\phi_1=1} \quad \text{(B.20)}$$

Appendix C

In this paper and ref 14 we assumed

$$r_1^0 v_1^* = r_i v^* \quad \text{(C.1)}$$

and

$$\sum_{i=1} r_i^0 N_i = \sum_{i=1} r_i N_i = rN \quad \text{(C.2)}$$

Combining eq C.1 and C.2 yields

$$v^* = \sum \phi_i^0 v_i^* \quad \text{(C.3)}$$

where

$$\phi_i^0 = r_i^0 N_i / rN \quad \text{(C.4)}$$

Our first assumption implied that the number of sites occupied by a molecule of species i in the mixture differed from that in the pure state. This artifice guarantees simple additivity of the close-packed (CP) volumes (see eq 20).

To make the theory more general we replace assumption C.1 with

$$r_i = r_i^0 \quad \text{(C.5)}$$

That is, a molecule of species i occupies the same number of sites in the mixture as it does in the pure state. The CP volume of the mixture, V^*, is now, in general, not equal to the sum of the pure component CP volumes:

$$V^* = \sum(r_i^0 N_i)v^* = rNv^* \neq \sum r_i^0 N_i v_i^* \quad \text{(C.6)}$$

The fraction of sites, f_i, occupied by species i is now given by

$$f_i = \frac{r_i^0 N_i}{rN + N_0} = \tilde{\rho}\phi_i^0 \quad \text{(C.7)}$$

where, as before, $\tilde{\rho}$ is the total fraction of occupied sites

$$\tilde{\rho} \equiv \frac{rN}{rN + N_0} \quad \text{(C.8)}$$

With eq C.5 it is unnecessary to define a CP volume fraction, ϕ_i (see eq 27 and 32). In all subsequent equations below the superscript 0 is omitted on ϕ_i^0 and r_i^0; it is understood that $\phi_i = \phi_i^0$ is a *site fraction* given by

$$\phi_i \equiv r_i N_i / rN = (m_i/\rho_i^* v_i^*) / \sum_i (m_i/\rho_i^* v_i^*) \quad \text{(C.9)}$$

Compared to the CP state the entropy of the LF is

$$S = -k \sum_{i=0} N_i \ln f_i \quad \text{(C.10)}$$

or

$$S/rN = -K \left\{ (\tilde{v} - 1) \ln(1 - \tilde{\rho}) + \frac{1}{r} \ln \tilde{\rho} + \sum_{i=1} \frac{\phi_i}{r_i} \ln \phi_i \right\} \quad \text{(C.11)}$$

where the ϕ_i in eq C.11 are defined by eq C.9.

Generalization of eq 13 and 14 to multicomponent mixtures yields the following for the configurational potential energy, E:

$$E/V = \frac{1}{2}\sum\sum\rho_i\rho_j \int \epsilon_{ij}(\mathbf{R})g_{ij}(\mathbf{R}) \, d\mathbf{R} \quad \text{(C.12)}$$

where ρ_i is the number of mers of type i per unit volume:

$$\rho_i \equiv r_i N_i / V = f_i/v^* = \tilde{\rho}\phi_i/v^* \quad \text{(C.13)}$$

Again we assume that the mers have hard cores and interact attractively with one another at a distance R via an inverse power law; i.e.,

$$\epsilon_{ij}(R) = \infty \text{ for } R/\sigma_{ij} < 1$$
$$\epsilon_{ij}(\mathbf{R}) = -\epsilon_0^{ij}(\sigma_{ij}/R)^n \text{ for } R/\sigma_{ij} > 1 \quad \text{(C.14)}$$

where σ_{ij} is the closest distance of approach allowed between mers i and j. Of course, for the diagonal terms

$$\sigma_{ii}^3 = v_i^* \quad \text{(C.15)}$$

In the mean field approximation, the pair distribution function, $g_{ij}(\mathbf{R})$, is given by

$$g_{ij}(R) = 0 \text{ for } R/\sigma_{ij} < 1$$
$$g_{ij}(R) = 1 \text{ for } R/\sigma_{ij} > 1 \quad \text{(C.16)}$$

Substitution of eq C.13, C.14, and C.16 into eq C.12 yields

$$E = -rN\tilde{\rho}\epsilon^* \quad \text{(C.17)}$$

where

$$\epsilon^* \equiv \frac{1}{v^*}\sum_i\sum_j \phi_i\phi_j\epsilon_{ij}^*\sigma_{ij}^* \quad \text{(C.18)}$$

$$\epsilon_{ij}^* = 2\pi\epsilon_0^{ij}/(n-3) \quad \text{(C.19)}$$

Up to this point we have only invoked one combining rule, namely eq C.5, and have left v^*, the average CP volume of a mer in the mixture, undefined. We now assume that v^* is given by

$$v^* = \sum_i\sum_j \phi_i\phi_j\sigma_{ij}^3 \quad \text{(C.20)}$$

Two more combining rules must be specified for the cross terms σ_{ij} and ϵ_{ij}. This is an old problem familiar to those who have studied the properties of fluid mixtures. Usually they are given by the semiempirical Lorentz–Berthelot rules:

$$\epsilon_{ij} = (\epsilon_{ii}\epsilon_{jj})^{1/2}$$
$$\sigma_{ij} = (\sigma_{ii} + \sigma_{jj})^{1/2} \quad \text{(C.21)}$$

However, there are many other combinations that have been considered [see, for example, R. J. Good and C. J. Hope, *J. Chem. Phys.*, **55**, 111 (1971)].

If eq C.21 were adopted, or some other equivalent expressions, the properties of a multicomponent mixture would be completely determined by the properties of the pure components. This prospect seems unlikely so it will be necessary to introduce one or more empirical parameters. For example, we could assume

$$\epsilon_{ij} = \zeta(\epsilon_{ii}\epsilon_{jj})^{1/2}$$
$$\sigma_{ij} = \xi(\sigma_{ii} + \sigma_{jj})/2 \quad \text{(C.22)}$$

where ζ and ξ are dimensionless constants. It is in this general area of combining rules that the LF theory is very flexible. By comparing calculated and experimental mixture properties for a large number of binary mixtures, it may be possible to determine the optimum set of combining rules.

Finally, it is worth mentioning that simple additivity of CP volumes is obtained for

$$\sigma_{ij}^3 = (\sigma_{ii}^3 + \sigma_{jj}^3)/2 \qquad (\text{C}.23)$$

Using this rule for σ_{ij} it can be shown that ϵ^* is given by eq 36.

References and Notes

(1) P. I. Freeman and J. S. Rowlinson, *Polymer*, 1, 20 (1960).
(2) P. J. Flory, R. A. Orwoll, and A. Vrij, *J. Am. Chem. Soc.*, 86, 3515 (1964).
(3) P. J. Flory, *J. Am. Chem. Soc.*, 87, 1833 (1965).
(4) B. E. Eichinger and P. J. Flory, *Trans. Faraday Soc.*, 64, 2035 (1968).
(5) P. J. Flory, *Discuss. Faraday Soc.*, 49, 7 (1970).
(6) D. Patterson, *J. Polym. Sci., Part C*, 16, 3379 (1968).
(7) D. Patterson, *Macromolecules*, 2, 672 (1969).
(8) D. Patterson and G. Delmas, *Discuss. Faraday Soc.*, 49, 98 (1970).
(9) J. Biros, L. Zeman, and D. Patterson, *Macromolecules*, 4, 30 (1971).
(10) I. Prigogine, "The Molecular Theory of Solutions", North-Holland Publishing Co., Amsterdam, 1957, Chapter XVI.
(11) P. J. Flory, "Principles of Polymer Chemistry", Cornell University Press, Ithaca, N.Y., 1953, Chapter 12.
(12) I. C. Sanchez and R. H. Lacombe, *J. Phys. Chem.*, 80, 2352 (1976).
(13) I. C. Sanchez and R. H. Lacombe, *J. Polym. Sci., Polym. Lett. Ed.*, 15, 71 (1977).
(14) R. H. Lacombe and I. C. Sanchez, *J. Phys. Chem.*, 80, 2568 (1976).
(15) J. D. Bernal, "Liquids Structure, Properties, Solid Interactions",

T. J. Hughel, Ed., Elsevier, Amsterdam, 1965.
(16) R. N. Howard, "Physics of Glassy Polymers", R. N. Haward, Ed., Wiley, New York, N.Y., 1973, p 39.
(17) J. M. Bardin and D. Patterson, *Polymer*, 10, 247 (1969).
(18) G. Delmas, D. Patterson, and T. Somcynsky, *J. Polym. Sci.*, 57, 79 (1962).
(19) P. J. Flory, J. L. Ellenson, and B. E. Eichinger, *Macromolecules*, 1, 279 (1968).
(20) B. E. Eichinger and P. J. Flory, *Trans. Faraday Soc.*, 64, 2061 (1968).
(21) B. E. Eichinger and P. J. Flory, *Trans. Faraday Soc.*, 64, 2053 (1968).
(22) A. H. Liddell and F. L. Swinton, *Discuss. Faraday Soc.*, 49, 115 (1970).
(23) The exact numerical value of χ, or its enthalpic and entropic components χ_H and χ_S, will depend on how ϕ is defined (volume fraction, site fraction, etc.). Usually the differences are less than 10%. The experimental values of χ_1, $\chi_{H;1}$, and $\chi_{S;1}$ tabulated in Table IV were taken from ref 5 where ϕ was defined as a "segment fraction". This definition closely corresponds to the LF definition of ϕ given by eq 32.
(24) B. E. Eichinger and P. J. Flory, *Trans. Faraday Soc.*, 64, 2066 (1968).
(25) S. Saeki, N. Kuwahara, S. Konno, and M. Kaneko, *Macromolecules*, 6, 246, 589 (1973).
(26) S. Saeki, S. Konno, N. Kuwahara, M. Nakata, and M. Kaneko, *Macromolecules*, 7, 521 (1974).
(27) S. Saeki, N. Kuwahara, and M. Kaneko, *Macromolecules*, 9, 101 (1976).
(28) C. E. H. Bawn and M. A. Wajid, *Trans. Faraday Soc.*, 44, 1658 (1956).
(29) P. J. Flory and H. Hocker, *Trans. Faraday Soc.*, 67, 2258 (1971).

Compositional Variation of Glass-Transition Temperatures. 2. Application of the Thermodynamic Theory to Compatible Polymer Blends

P. R. Couchman

Department of Mechanics and Materials Science, Rutgers University, Piscataway, New Jersey 08854. Received May 22, 1978

ABSTRACT: The characteristic continuity of extensive thermodynamic parameters at glass-transition temperatures forms the basis for a theory to predict T_g in intimate mixtures of compatible high polymers from pure-component properties. A relation derived from the mixed system entropy in terms of pure component heat capacity increments and glass-transition temperatures is shown to arise as a consequence of the connectivity constraint on the excess mixing entropy in these blends. Four known essentially empirical relations for the effect, including a predictive version of the Wood equation, are obtained as special cases of this expression. A second mixing relation is derived in terms of pure component properties from the volume continuity condition at T_g. Quantitative restrictions on excess mixing volumes associated with this relation suggest that the entropic expression may be of wider use. The derivation of relations for the effect of pressure on T_g is touched on. Finally, for two related blends, the entropy-based relation is shown to predict glass-transition temperatures in very good agreement with experimental values.

The prediction of glass-transition temperatures in compatible mixtures from pure-component properties presents a problem of some technological and scientific interest. Plasticized polymers and polymer blends find a wide variety of industrial applications; however, the compositional variation of glass-transition temperatures in these mixtures is generally discussed in terms of essentially empirical expressions.[1] The physically plausible "free volume" hypothesis has provided a rationalization of certain of these relations.[1-4] Separately, a statistical mechanical interpretation of composition effects on T_g has been given in terms of the DiMarzio–Gibbs "configurational" entropy hypothesis of glass formation.[5]

The first of these approaches is known to offer some basic difficulties and can lead to relations which are inconsistent with experimental evidence, while the DiMarzio–Gibbs method does not appear to provide an explicit expression for T_g in terms of composition. A quasi-macroscopic form of the configurational entropy hypothesis of glass formation has been applied recently to the problem in ideal and regular solutions[6] but, necessarily, is couched in terms of fictive rather than actual transition temperatures. Its application to mixtures thus necessitates knowledge of the fusion entropy for each pure component, assumes the compositional variation of fictive transition temperatures to reproduce that of T_g, and re-